Impacts of Merging Profiler and Rawinsonde Winds on TOGA COARE Analyses

PAUL E. CIESIELSKI

Department of Atmospheric Science, Colorado State University, Fort Collins, Colorado

LESLIE M. HARTTEN

Cooperative Institute for Research in Environmental Sciences/NOAA Aeronomy Laboratory, Boulder, Colorado

RICHARD H. JOHNSON

Department of Atmospheric Science, Colorado State University, Fort Collins, Colorado

(Manuscript received 27 September 1996, in final form 15 February 1997)

ABSTRACT

During the intensive observing period of the Tropical Ocean Global Atmosphere Coupled Ocean–Atmosphere Response Experiment, a large number of collocated rawinsonde and profiler wind observations were taken at six Integrated Sounding System (ISS) sites and Biak, Indonesia. To mitigate limitations in the rawinsonde dataset due to missing and bad wind observations, a procedure was developed to combine profiler and sonde winds to produce an integrated, high-quality, upper-air sounding dataset. In addition to improving the overall quality of the winds, this procedure eliminates several data gaps in the sonde dataset. For example, below 800 hPa the amount of bad and missing wind data is reduced from about 45% to 20% at the land-based ISS sites.

This paper describes the procedure for combining sonde and profiler winds into a single, coherent merged dataset. Examining the impact of this merger upon various atmospheric analyses, the authors find that inclusion of profiler winds results in some substantial changes in the analyses, particularly on daily to weekly timescales. To assess whether these changes are an improvement, budget-derived rainfall estimates from analyses with and without profiler winds are compared to Special Sensor Microwave/Imager satellite-based estimates. Overall, this comparison shows that inclusion of profiler winds into the sonde dataset has a beneficial impact upon the analyses.

Information for accessing the merged datasets for the seven sites considered in this paper via the Internet is described.

1. Introduction

The Tropical Ocean Global Atmosphere (TOGA) Coupled Ocean–Atmosphere Response Experiment (COARE) has provided researchers with an unprecedented dataset of atmospheric and oceanic variables over the globally important warm pool. During the intensive observing period (IOP) of COARE (November 1992–February 1993), a network of upper-air sounding stations (shown in Fig. 1) was established over the western Pacific to determine the mesoscale to synoptic-scale structure of atmospheric circulation systems over the warm pool (Webster and Lukas 1992). This network consisted of nested arrays, ranging from the large scale array (LSA) on the synoptic scale with twice-per-day soundings, to the outer sounding array (OSA) and intensive flux array (IFA) on the subsynoptic or mesoscale with four-per-day soundings. Extensive efforts have been made by the Joint Office for Science Support (JOSS) to postprocess and quality control these atmospheric soundings (Loehrer et al. 1996).

As an enhancement to the atmospheric rawinsonde network shown in Fig. 1, six Integrated Sounding Systems (ISS) were deployed within the LSA—four land based and two ship based. Four of these ISS sites (Kapingamarangi or Kapinga, Kavieng, R/V *Shiyan #3,* and R/V *Kexue #1*) were located at the vertices of the IFA polygon, which as its name implies was the focus of intensive observations during the IOP. In addition, three of the ISS sites (Manus, Kapinga, and Nauru) were part of the enhanced monitoring array (EMA), which was established to monitor the progression of the intraseasonal oscillation over the COARE domain. Each ISS was equipped with a surface meteorological station, an acoustic sounder, a 915-MHz wind profiler, and an OMEGA NAVAID-based rawinsonde system. The ISS was designed with the idea that the individual measurement systems would complement each other by

Corresponding author address: Paul E. Ciesielski, Department of Atmospheric Science, Colorado State University, Fort Collins, CO 80523-1371.
E-mail: paulc@tornado.atmos.colostate.edu

© 1997 American Meteorological Society

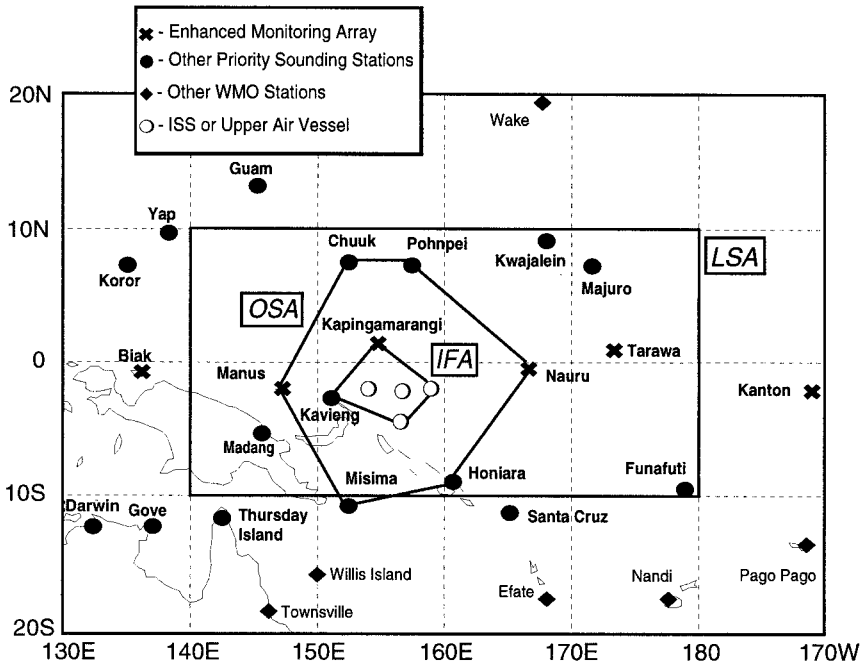

FIG. 1. The TOGA COARE sounding network showing the location of the intensive flux array (IFA), the outer sounding array (OSA), and the large-scale array (LSA).

taking advantage of each system's positive attributes (Parsons et al. 1994). The necessity of such an approach is apparent when one examines the ISS rawinsonde dataset, which contains a significant amount of bad or missing wind data due to problems and deficiencies with the OMEGA-sounding system. In this paper we demonstrate that much of this data loss can be mitigated by utilizing high temporal resolution profiler winds. In addition, a 50-MHz profiler was operated in a high-height mode at Biak, Indonesia. Profiler data from this site are also used to supplement the rawinsonde winds at Biak that at times were of questionable quality during the IOP.

A fundamental goal of COARE is to attempt to quantify air–sea fluxes of sensible heat, latent heat, and momentum. These fluxes can be computed as budget residuals using data obtained from the rawinsonde network described above. Preliminary estimates of budget-derived IOP–IFA average rainfall presented at the Joint Workshop of the Flux and Atmospheric Groups on 11–13 July 1995 showed discrepancies of nearly a factor of 2 using different analytical techniques (Bradley and Weller 1995). We will demonstrate that inclusion of profiler winds improves the quality of upper-air soundings, particularly in the lower troposphere, thereby improving budget estimates of fluxes and precipitation that are sensitive to divergence calculations.

This paper describes our efforts to merge rawinsonde and profiler winds to produce the most complete, high-quality, upper-air sounding dataset possible. Section 2 examines the characteristics and performance of the sonde and profiler systems at the ISS sites and Biak during the IOP. Our procedure for merging profiler and sonde winds into a single coherent dataset is described in section 3. Next in section 4, we compare mean wind profiles from the sonde-only and merged datasets. In section 5 we examine the impacts of using this merged dataset on various circulation fields and derived quantities, such as vertical motion and budget-derived precipitation. Finally, information for accessing the merged dataset via the Internet using the World Wide Web (WWW) is presented along with some concluding remarks in section 6.

2. Characteristics and performance of sonde and profiler systems

a. ISS sites

The ISS used a rawinsonde system configured to use OMEGA navigational signals in computing the horizontal wind. Details of this system and the processing of the sonde data are contained in Miller and Riddle (1994). Major sources of error in OMEGA-derived wind estimates are discussed in Franklin and Julian (1984). In this paper they classify OMEGA system wind-finding errors as either ''external'' (e.g., phase modal interference, sudden ionospheric disturbances) or ''internal'' (e.g., sonde-transmitter geometry, choice of phase-smoothing algorithm). From the OMEGA system, wind values were computed every 10 s using a centered sliding window smoothing technique over a 240-s smoothing interval. As a consequence of this technique, the first calculated wind occurred approximately 120 s after sonde launch. With a typical balloon ascent

rate of 5 m s^{-1}, the first computed wind was usually around 600 m. Between this level and the surface, where winds are measured by an independent surface observation, wind data were filled in by linear interpolation (subject to the constraints described in the following paragraph). The final processed sonde winds with attendant thermodynamic data were made available to the community by the National Center for Atmospheric Research Atmospheric Technology Division (NCAR/ATD) in two formats: a 10-s data stream or a set of interpolated values at constant pressure increments of 5 hPa. For convenience, we use the interpolated dataset in this study. We have, however, substituted NOAA's Aeronomy Lab (AL) processed ISS surface winds (Hartten 1997) for the ship-based surface winds provided by ATD in all the work presented here.

The wind algorithm used by ATD also returns quality parameters (or *Q* values) with units of meters per second, which are the standard deviations of wind estimates from the smoothing interval for their calculation. As a statistical parameter, *Q* values contain information concerning both signal noise and meteorological variability. To separate this information would be extremely difficult, if not impossible. In general though, low (high) *Q* values signify good (bad) data. Exceptions to this are possible in regions of strong wind shear when good data could result in high *Q* values. Conversely, long periods of consistently bad wind data were occasionally noted to produce low *Q* values. Wind values in the 5-hPa interpolated dataset were computed from 10-s data that met a noise limit constraint of $Q \leq 2$. If the interpolation interval was less than or equal to 50 s, the *Q* value in the interpolated dataset represents the standard error estimate. On the other hand, if the interpolation interval was between 50 and 100 s, the winds were interpolated but flagged with a *Q* value of 88. If the interpolation interval was longer than 100 s (as in the near-surface layer) the winds were considered bad and were flagged with a *Q* value of 99. In this case, the winds determined by the interpolation were kept if the interpolation interval was less than 100 hPa, otherwise they were set to 999.0 (the value used to indicate bad or missing winds). Missing wind data at higher altitudes were usually due to difficulty in obtaining a radionavigational lock. Data from the surface observation were assigned a *Q* value of 77. In summary, the ISS datasets used in this study (from the original postprocessed ATD release) follow the convention that *Q* values less than or equal to 2 are continuous and statistical in nature, while above this value they are discrete and descriptive in nature.

The accuracy of winds obtained from the OMEGA system is dependent on several factors: the number of stations from which an OMEGA signal is received (three is the minimum), the strength of the signal, and the geometry of the receiver with respect to the station. The performance of the OMEGA systems at sampling the wind is depicted in Fig. 2, which shows the time and altitude of sonde wind measurements with $Q \leq 1$ plotted over the range of pressures at which profiler data are also generally present. The most glaring deficiency in data coverage noted in these plots occurs below 940 hPa where, due to the wind smoothing algorithm, processed sonde winds are seldom present. This information is summarized in Tables 1 and 2, which give the percentage of bad or missing sonde wind data at the ISS sites below and above 500 hPa, respectively. Over the course of the IOP this percentage ranges from 15% to 25% below 500 hPa and less than 10% above this level. The most notable exception to this occurred at Kapinga from December through early January when a significantly higher percentage of data was lost. Much of this data loss occurred at lower levels due to difficulty in obtaining a prelaunch OMEGA lock (H. Cole 1996, personal communication). This problem was traced to an improper launch configuration OMEGA antenna and improved substantially after 10 January 1993. If one considers from the surface to 800 hPa, the rate of missing sonde winds averaged approximately 45% at the ISS sites with a maximum data loss rate of 72% at Kapinga in December.

To complement the radiosonde network, an array of 915-MHz wind profilers were deployed at the six ISS sites.[1] These profilers, operating as a Doppler beam swinging system, measured radial wind velocities from a few hundred meters to several kilometers above the surface. The exact vertical extent of measurements with these profilers varies with meteorological conditions and specified parameters such as power and pulse length. In the Tropics typical vertical ranges are 5–6 km in clear air conditions and twice that during rain (Carter et al. 1995). During the IOP, half-hour average winds were computed for two vertical modes: a low mode with a 98-m vertical resolution and a high mode with a 238-m resolution. The lowest altitudes for which reliable winds were available were approximately 300 m at Kavieng, Manus, and Nauru; approximately 400 m at Kapinga; and approximately 700 m on the two ships. Below these levels, winds were considered unreliable due to dynamic range limitations, receiver recovery issues, and sea clutter problems at Kapinga and the ships (Riddle et al. 1996; Hartten 1997). The profiler data were processed on site into ''quick-look'' winds by the computers controlling the radar. Upon completion of the IOP, the original spectral data underwent a two-step postprocessing that included time and space consistency checks; this resulted in the final released set. The original spectral data from Nauru were lost for much of the IOP. While quick-look data were available at Nauru for much of this period (see Fig. 3), they are not used in this study due to deficiences (i.e., questionable winds, particularly above 5 km) in this dataset. Details of the profiler configuration and processing are contained in Riddle et al. (1996). The final profiler dataset released by NOAA's AL contains, in addition to horizontal and vertical wind components, a variety of parameters that can be used to eval-

[1] A 915-MHz profiler was also deployed on R/V *Moana Wave* during the IOP. However, problems with this profiler, which are documented in Riddle and Miller (1994), resulted in no reliable winds.

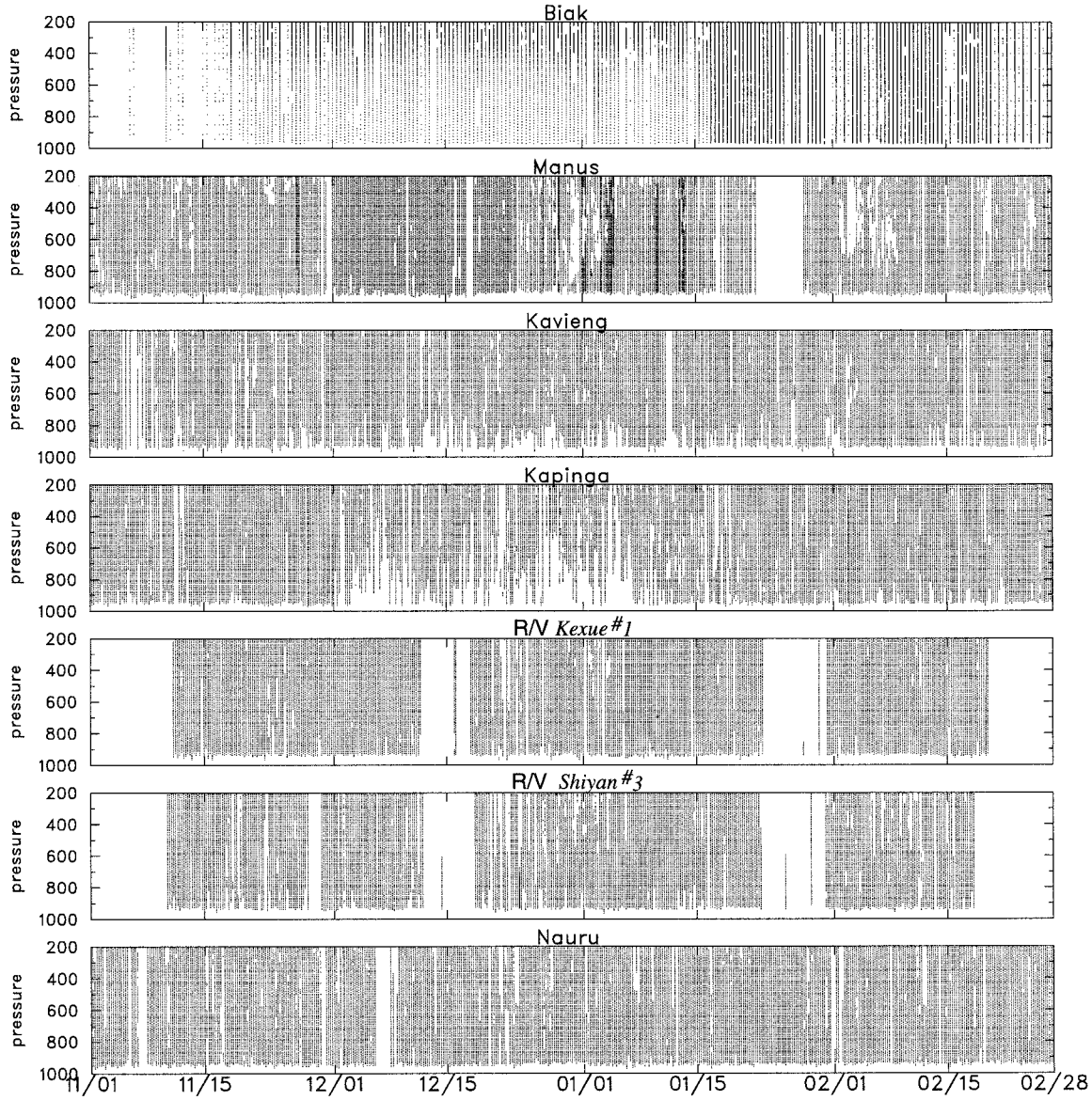

FIG. 2. Visual inventory of sonde wind data at Biak and ISS sites. Each dot depicts the time and altitude of a measurement with a QC flag less than or equal to 1.

TABLE 1. Percent of wind data from the surface to 500 hPa that is either missing or bad in the sonde and merged (in parentheses) datasets for sondes launched during the IOP. Percentages do not include periods when no sondes were launched for whatever reason (e.g., ships in port, instrument problems).

ISS site	November	December	January	February
Kapinga	17.7 (10.2)	46.1 (12.5)	29.6 (11.1)	15.0 (9.3)
Kavieng	23.1 (9.4)	26.3 (11.0)	22.8 (8.2)	22.4 (8.2)
Manus	15.6 (6.9)	20.5 (7.9)	20.1 (7.0)	23.5 (9.1)
Nauru	15.5 (15.5)	15.4 (10.0)	13.7 (12.7)	15.6 (15.5)
R/V *Kexue #1*	17.1 (13.3)	17.5 (13.7)	16.0 (13.7)	15.0 (13.2)
R/V *Shiyan #3*	20.3 (16.3)	20.4 (17.3)	18.6 (15.3)	19.3 (15.0)

uate the reliability of the winds (Riddle et al. 1996). In this study, profiler winds were used only if the following criteria were satisfied:

- quality flag less than 4 (range is 0 to 9),
- at least 2 triad scans[2] (out of a possible 7 or 8) per half hour, and

[2] Each profiler scans the atmosphere along three beams: one vertical and two oblique. Each set of consecutive scans of those three beams is called a triad.

TABLE 2. Percent of wind data from 500 to 100 hPa that is either missing or bad in the sonde and merged (in parentheses) datasets for sondes launched during the IOP. Percentages do not include periods when no sondes were launched for whatever reason (e.g., ships in port, instrument problems).

ISS site	November	December	January	February
Kapinga	2.9 (2.7)	8.0 (7.9)	8.8 (8.3)	2.0 (1.6)
Kavieng	7.0 (4.8)	3.0 (2.3)	2.3 (1.9)	4.5 (4.1)
Manus	13.9 (13.4)	6.3 (5.8)	16.3 (14.0)	19.8 (17.5)
Nauru	4.3 (4.3)	5.4 (3.3)	4.5 (4.5)	3.9 (3.9)
R/V *Kexue #1*	2.7 (2.2)	3.1 (1.9)	4.5 (3.8)	3.3 (2.2)
R/V *Shiyan #3*	1.8 (1.7)	6.8 (6.8)	2.6 (2.4)	5.1 (4.7)

- spectral width less than 3 m s^{-1} in each oblique beam.

The quality flag is derived from internal consistency checks or known instrument problems and thus does not give any information about the quality with respect to the physics involved. Riddle et al. (1996) suggest that values less than 4 are likely to indicate good data. The second criterion requires that at least two full wind measurements were used to compute the half-hour averaged wind, while the third criterion filters false echoes in the data from R/V *Shiyan #3* that were caused by a faulty chip. The ability of the profilers to sample the horizontal wind components in high mode is depicted in Fig. 3, which shows the time and altitude of profiler wind mea-

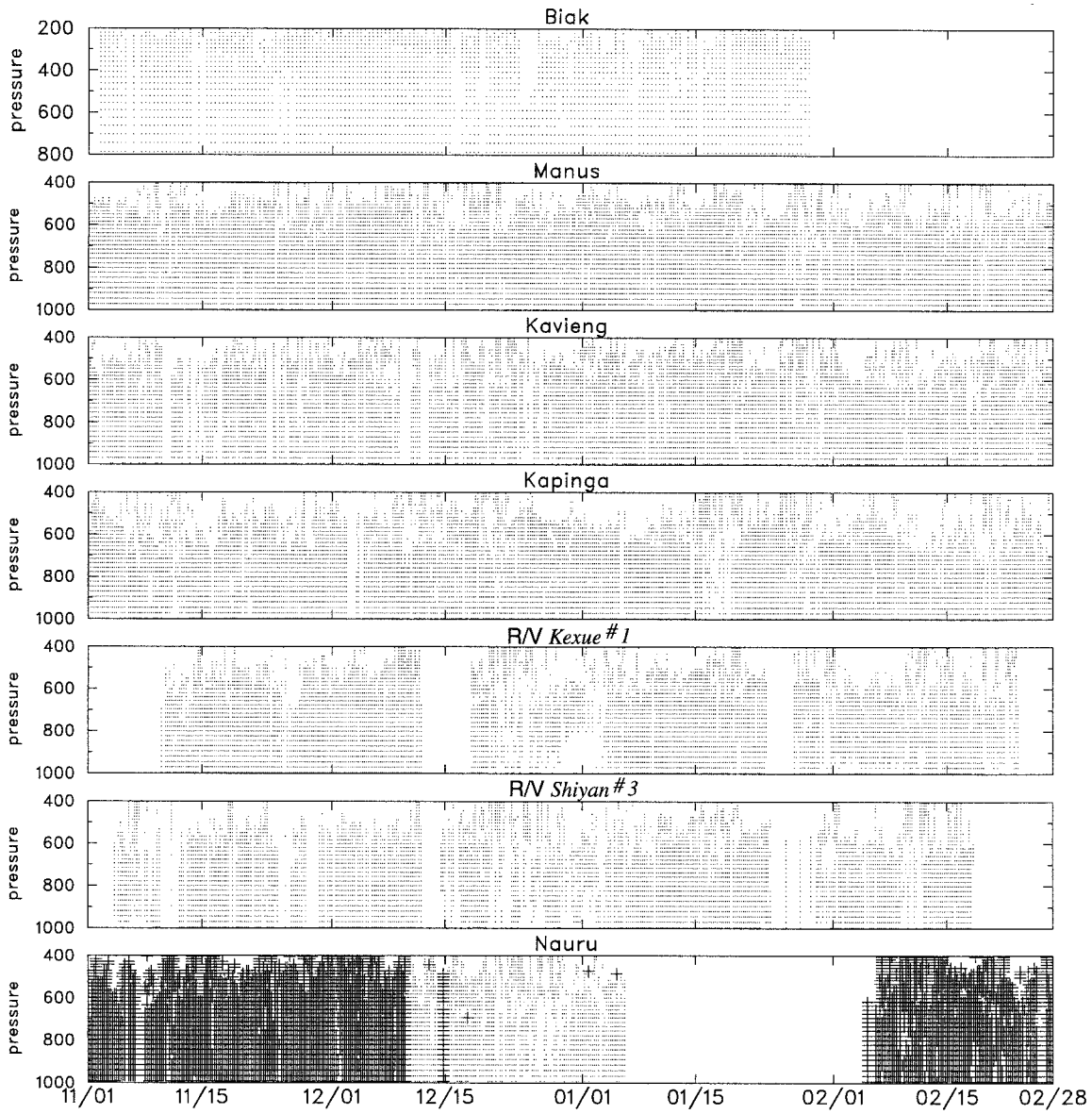

FIG. 3. Visual inventory of profiler high-mode wind data that was taken within half an hour of sonde launches at Biak and ISS sites. Each dot depicts the time and altitude of a reliable measurement from the postprocessed dataset (see text for details). For Nauru only, each plus sign (which may appear as darker shading) depicts the time and altitude of a measurement from the quick-look dataset.

surements that are within half an hour of sonde launches and satisfy the criteria described above. From this diagram one can see that the data coverage provided by the profilers at the ISS sites is reasonably good between the surface and 500 hPa, except at Nauru.

b. Biak site

Biak, Indonesia (1.1°S, 136.1°E), also had wind profiler and rawinsonde capabilities during the COARE IOP. Due to its prominent location near the equator and the western boundary of the LSA, Biak was designated as part of the EMA for COARE. The Biak site, which launched VIZB rawinsondes at 0000 and 1200 UTC, used a radiotheodolite windfinding system. An intensive postprocessing effort was made to produce the highest quality sounding dataset possible for Biak. Recomputation of winds included digitizing azimuth and elevation angles from strip charts. Despite these efforts nearly 20% of the reprocessed Biak wind data were judged as bad or questionable by the spatial quality control procedures of JOSS. Unlike the ISS sonde quality flags from the ATD dataset that have a statistical basis, those at Biak are more physical in nature. Based on quality control procedures at JOSS, Biak sonde data were judged to be good, questionable, or bad and were assigned a quality value of 1, 2, or 3, respectively. The presence of reliable sonde wind data ($Q = 1$) at Biak is shown in Fig. 2, which shows a considerable amount of missing or poor quality wind data early in the IOP. Also note in Fig. 2 that the vertical resolution of the Biak sonde data increased from approximately 150 m (30 s) prior to January 17 to approximately 30 m (6 s) after this date.

The profiler at Biak was a VHF 50-MHz profiler. It operated in a high-height coverage with measurements at 48 heights and a vertical resolution of 480 m. Severe radio interference problems at Biak during the IOP resulted in questionable winds above 13 km. Although the Biak profiler operated from July 1992 through June 1993, no data were available in February 1993, as is seen in Fig. 3.

3. Merging procedure

The procedure for producing a merged dataset of sonde and profiler winds is outlined here. To ensure temporal coherency between the datasets, sonde and profiler winds were merged together only if their observation times were within half an hour of each other. In this case, prior to merging the two datasets, reliable profiler winds were interpolated to the pressure levels of sonde data to achieve a resolution consistent with this dataset. To perform this interpolation we first transformed the profiler data, which are provided as a function of height, into a function of pressure using the IOP-mean pressure–height relationship computed from the sonde data at each site. This transformation is quite accurate because of the invariant nature of pressure fields in the Tropics. For Biak the pressure levels for interpolation varied for each sonde, while for the ISS sites interpolation was done at constant pressure increments of 5 hPa. On the other hand, if a sonde launch was missed for whatever reason but profiler data existed at the usual sonde launch time, the profiler data were entered into the merged dataset at their native resolution.

a. ISS sites

At the surface, the wind value from the sonde dataset is entered into the merged dataset except at the ships, where the AL-reprocessed wind value is used. Above the surface, creation of the merged dataset for the ISS sites considers the following four cases.

1) If neither reliable profiler winds nor sonde winds with $Q \leq 1$ are available at a particular level and time, the value 999.0 is entered for the wind in the merged dataset.
2) If only sonde wind data with $Q \leq 1$ are available at a particular level and time, they are entered into the merged dataset. It was our subjective determination that winds with $Q > 1$ were typically bad and thus were not used in this study.
3) If only profiler winds are available at a particular level and time, they are entered into the merged dataset if they are considered reliable (i.e., they satisfy the quality control criteria described in previous section).
4) If reliable profiler and sonde winds are both present at a particular level and time, the wind entered into the merged data is a weighted average of the two winds. This averaging is shown here for the u component of the wind:

$$u_m = 0.5[(1 - Q_u)u_s + (1 + Q_u)u_p], \qquad (1)$$

where

u_m is the merged u component (m s^{-1})

u_s is the sonde u component (m s^{-1})

u_p is the profiler u component (m s^{-1})

Q_u is the quality flag for the u component sonde data; however, if $Q_u > 1$, then Q_u is reset to 1 in (1).

The rationale behind this simple weighting scheme is as follows. Profiler winds are considered to be reliable if they satisfied the quality control criteria outlined in the previous section. On the other hand, reliability of sonde winds is quantified in terms of their Q values, which measure the wind's vertical coherency. In this scenario, sonde winds are considered to be of comparable reliability to profiler winds as their Q values approach 0. Sonde wind Q values typically ranged between 0.0 and 0.2 under most wind conditions; however, as Q values approached 1.0, reliability of the measured wind

TABLE 3. Code and description of quality control flags used in the merged datasets for the ISS sites.

Code	Description
0–1	Sonde data
10	Profiler data (low mode)
11	Profiler data (high mode)
12	Merged sonde–profiler data (low mode)
13	Merged sonde–profiler data (high mode)
77	Surface data
88	Interpolated sonde data
99	Missing data

TABLE 4. Number of wind profiles in the merged dataset.

Site	Generated from profiler winds in absence of sonde launches	Generated from both sonde and profiler winds	Total
Biak	1	145	239
Kapinga	5	481	496
Kavieng	11	443	483
Manus	29	464	494
Nauru	5	107	467
R/V *Kexue #1*	5	343	355
R/V *Shiyan #3*	3	321	353

decreases significantly. This weighting is shown here for a few Q values.

$$\text{If } Q_u = 0.0, \quad \text{then } u_m = 0.5(u_s + u_p).$$

$$\text{If } Q_u = 0.5, \quad \text{then } u_m = 0.25u_s + 0.75u_p.$$

$$\text{If } Q_u \geq 1.0, \quad \text{then } u_m = u_p.$$

Thus, the effect of this weighting scheme is to not use the sonde wind data if their Q values are greater than or equal to 1, but to use them with increasing weight as their Q values approach 0. This scheme also excludes all sonde winds that were computed via linear interpolation over layers of missing data, since their Q values equal 88 or 99.

An alternate and more sophisticated approach to computing merged wind estimates under case 4 would be optimal interpolation (Daley 1991), which uses error variances from both sonde and profiler winds. This approach is similar to the empirical formula defined in (1) in that winds are weighted according to their variance estimate (i.e., larger error variance leads to lower weighting of a wind estimate). Unfortunately, the optimal interpolation approach was not possible here due to the absence of error variance statistics in the profiler dataset.

Under cases 3 and 4, if data from both profiler modes are available, the low mode is used up to 1.5 km, while above this height the high mode is used. In this manner the low-mode data are used to resolve the planetary boundary layer, which is usually below 1.5 km. Above this level the signal-to-noise ratio of the low-mode data starts to decrease significantly with height, which warrants the use of the high-mode data.

Finally, a simple filtering scheme was designed to smooth over vertical discontinuities in the wind that resulted from using different instrument platforms at adjacent levels. Specifically, if the vertical shear exceeds 2 m s^{-1} per 5 hPa in a layer where the instrument platform changes (e.g., sonde wind at one level and a merged sonde–profiler wind at an adjacent level), a five-point running mean filter is applied to three 5-hPa-deep levels on either side of that layer.

The format of the merged dataset follows the generic CLASS format developed by NCAR/SSSF (Miller 1993) with the exception of some changes to the quality control (QC) flags. Since all wind estimates in the merged dataset are considered of good quality (the merged procedure having removed all bad winds), the QC flags in this dataset indicate the source of the winds, not their quality. As in Miller (1993) a QC flag of 99 denotes missing winds (case 1), while when sonde data are the sole source for the winds in the merged dataset (case 2), the QC flags are merely the Q values (ranging from 0.0 to 1.0) associated with the sonde winds. However, when the winds are generated solely from profiler data (case 3), the QC flags are assigned the value 10 or 11 to indicate that their source is low- or high-mode profiler winds, respectively. Similarly, when winds were computed from both sonde and profiler data (case 4), the QC flags are assigned the value 12 or 13 to indicate that their source is a combination of sonde winds and low- or high- mode profiler winds, respectively. The choice of QC flags (10–13) for cases 3 and 4 was to avoid any ambiguity with winds in the merged dataset generated from cases 1 and 2. The QC flags for the merged dataset at the ISS sites are summarized in Table 3.

The amount of missing or bad winds in the merged dataset are given by the percentages in parentheses in Tables 1 and 2. From the surface to 500 hPa this amount has been reduced to about 10% in the merged dataset at the land-based ISS sites. Below 800 hPa missing or bad winds have been reduced from approximately 45% in the sonde dataset to less than 20% in the merged. This reduction is less substantial at Nauru, which had final processed profiler winds for less than a quarter of the IOP, and at the two ships whose profiler winds were unreliable below 700 m. Above 500 hPa the merged procedure had a much smaller impact primarily due to the lack of profiler winds above this level. Unaccounted for in this table are the statistics for periods when profiler winds were entered into the merged dataset in the absence of sonde launches. The number of these occurrences are summarized in Table 4 along with the number of merged profiles generated at each site when both sonde and profiler winds were available. By using profiler winds in the absence of sonde launches, the large gap of missing winds at Manus in late January 1993 (see Fig. 2) was nearly eliminated in the merged dataset.

An example of how this procedure merges sonde and profiler data at a particular time (1200 UTC on 29 December 1992) and ISS site (Kapinga) is illustrated in

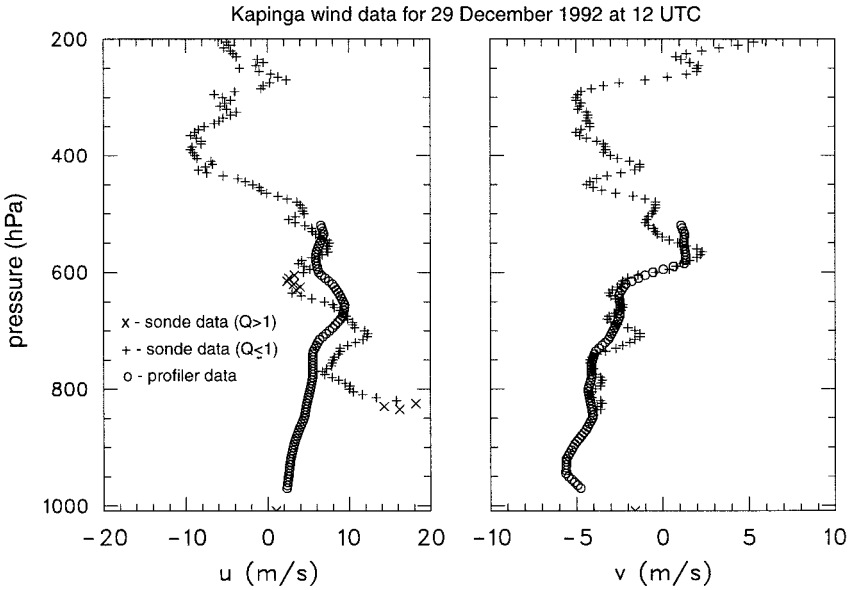

FIG. 4. Zonal and meridional components of the sonde and profiler winds for Kapinga at 1200 UTC 29 December 1992. The sonde winds with QC flags greater than 1 are plotted with the symbol "×," while sonde winds with QC flags less than or equal to 1 are plotted with the symbol "+." Profiler winds interpolated to every 5-hPa level (low mode below 1.5 km, high mode above) are plotted with the symbol "○."

Figs. 4 and 5. Figure 4 is a plot of the u and v wind components as a function of pressure from the profiler and sonde datasets. Two noteworthy features of the data present in this plot, and typical of other times and ISS sites, are the paucity of sonde winds at lower levels and of profiler winds above 500 hPa. As noted earlier, ISS sites typically did not have sonde winds below 600 m (~940 hPa); however, Kapinga during December and early January was especially prone to additional sonde wind data loss at low and midlevels. Although sonde data were present at midlevels in Fig. 4, their quality was relatively poor (i.e., $0.5 < Q_u < 1.5$) up to 550

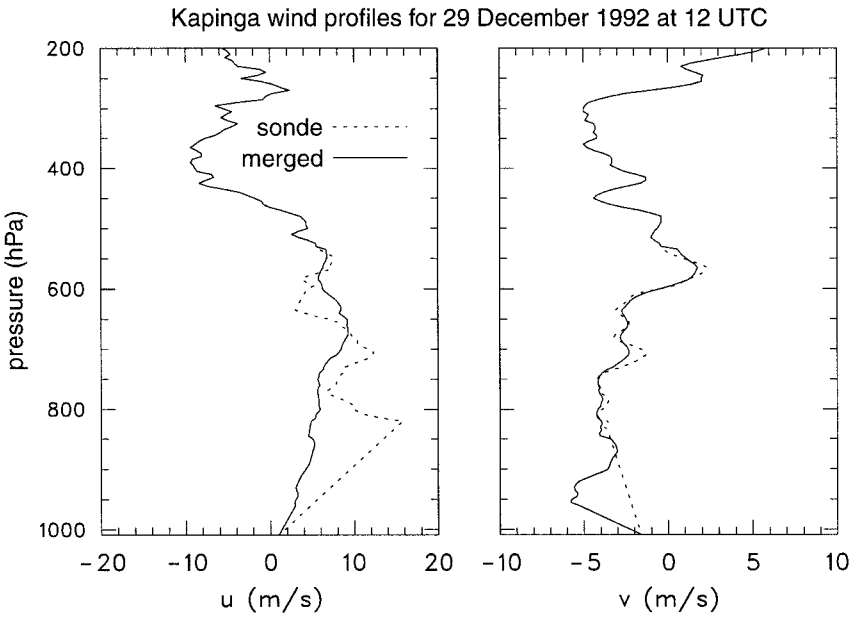

FIG. 5. Zonal and meridional wind profiles at Kapinga resulting from the merger of the sonde and profiler winds in Fig. 4 (solid line) and from only the sonde winds (dashed line). Missing winds were linearly interpolated in pressure.

hPa. Figure 5 shows the resulting merged profile (solid line) and the profile based solely on sonde winds (dashed line). In this case due to the low quality of the sonde winds, the merged profile closely resembles that of the profiler winds. The straight line below 800 hPa in the sonde wind profiles represents interpolation between the surface wind and the first available sonde wind with $Q \leq 1$. The large wind differences between the two profiles (> 10 m s^{-1} at some levels) show that the inclusion of profiler data can dramatically change the wind profile at a given time and location.

b. Biak site

Generation of a merged dataset at Biak is similar to that described above for the ISS sites with the following exceptions. Because of the difference in the nature of the QC flags at Biak, as discussed in section 2b, the merge procedure when both sonde and profiler winds are available is as follows (shown here for the u component of the wind).

$$\text{If } Q_u = 1.0, \quad \text{then } u_m = 0.5(u_s + u_p).$$
$$\text{If } Q_u > 1.0, \quad \text{then } u_m = u_p. \tag{2}$$

In other words, if $Q = 1$, the quality of the sonde wind is considered good so that the sonde and profiler winds are equally weighted in computing the merged wind. However, if the quality of the sonde wind is considered unreliable ($Q > 1$), the wind entered into the merged dataset is the profiler wind. Because of problems between incoming and outgoing beams (due to transmit/receive switch issues), profiler data are not used from its lowest two range gates (which, for the 50-MHz Biak profiler, are at 1686 and 2166 m). While no profiler winds are used below 2600 m at this site, the lower-level sonde winds at Biak are generally available and of good quality. In addition, the 50-MHz profiler at Biak was able to measure winds to much higher elevations (typically to 200 hPa) than the 915-MHz profilers at the ISS sites. The QC flags for the merged dataset at Biak follow the JOSS convention outlined in Table 2 of Loehrer et al. (1996), except for codes 10–13, which are listed in Table 3 of this paper.

4. Comparison of mean wind profiles

In comparing the sonde and profiler data it is important to bear in mind that the OMEGA sondes make point measurements that are vertically smoothed before being recorded, while profilers make volume-averaged measurements that are averaged in time before being recorded. Riddle et al. (1996) compared sonde and profiler winds at the ISS sites and found mean differences less than 1.0 m s^{-1}, except at higher altitudes where profiler data become less reliable (typically above 4.5 km for the low mode and 10.0 km for the high mode). In addition, they found that a significant portion of the difference, which tended to be larger in the zonal wind component, could be accounted for by occasional sondes that exhibited suspicious oscillatory structure in their winds at times when the profiler winds showed no such behavior. Riddle et al. (1996) stated that this wavelike structure in the sonde winds typically had vertical wavelengths of 0.5–2.0 km with typical peak-to-peak excursions of 5.0–10.0 m s^{-1} but occasionally exceeding 20.0 m s^{-1}. They attributed this behavior to tracking problems with the OMEGA system used by the sondes. In the reanalyzed set of sonde winds used in this study this oscillatory problem was largely eliminated.

Since the mean profiles at the various sites tend to share similar characters, we have chosen to show the statistics for Kapinga and R/V *Kexue #1,* which are the land- and ship-based sites with the largest number of merged profiles. The vector-mean wind speeds and directions taken from the merged dataset at these two sites are shown in Fig. 6. At these sites the mean was computed over all available merged profiles during the IOP (i.e., times when both profiler and sonde data were available). The number of merged profiles at each site is given in the third column of Table 4. The low number of available profiles for Nauru listed in Table 4 is due to the frequent absence of postprocessed profiler data (see Fig. 3). Where no merged data were produced due to the absence of either profiler or acceptable sonde data (e.g., in the lowest few hundred meters of the profiles), gaps were filled in by linear interpolation before these means were computed.

Over the course of the IOP, wind speeds were 1–3 m s^{-1} near the surface (stronger at sea than over land), usually reaching maximum speeds of 3–7 m s^{-1} between 700 and 900 hPa. There was frequently a relative minima near 400 hPa with speeds increasing again toward the tropopause, although at Kapinga the primary speed minima occurred near 600 hPa. These speed minima were near the level at which mean low-level westerlies became midtropospheric easterlies and the meridional wind was usually very light, if not actually switching sign, near this altitude. At the Southern Hemisphere sites, direction was roughly northwesterly at the surface, backing slightly with height to westerlies that extended to near 500 hPa, while at Kapinga the surface northwesterlies veered to northerlies by 950 hPa, then backed with height to westerlies that extended up to 600 hPa. At all stations the winds from 200 to 300 hPa were easterly. The lower-tropospheric results are similar to the vector-mean profiler winds presented in Gutzler and Hartten (1995), which also show low-level northwesterlies (northerlies at Kapinga) turning counterclockwise with height.

Also plotted in Fig. 6 are the wind profiles computed using the sonde dataset for the IOP released by NCAR/ATD, which includes interpolated wind components when no data were available (e.g., during the first 120 s of the balloon flight); these were the sonde winds used in the analysis of Lin and Johnson (1996). In the long-

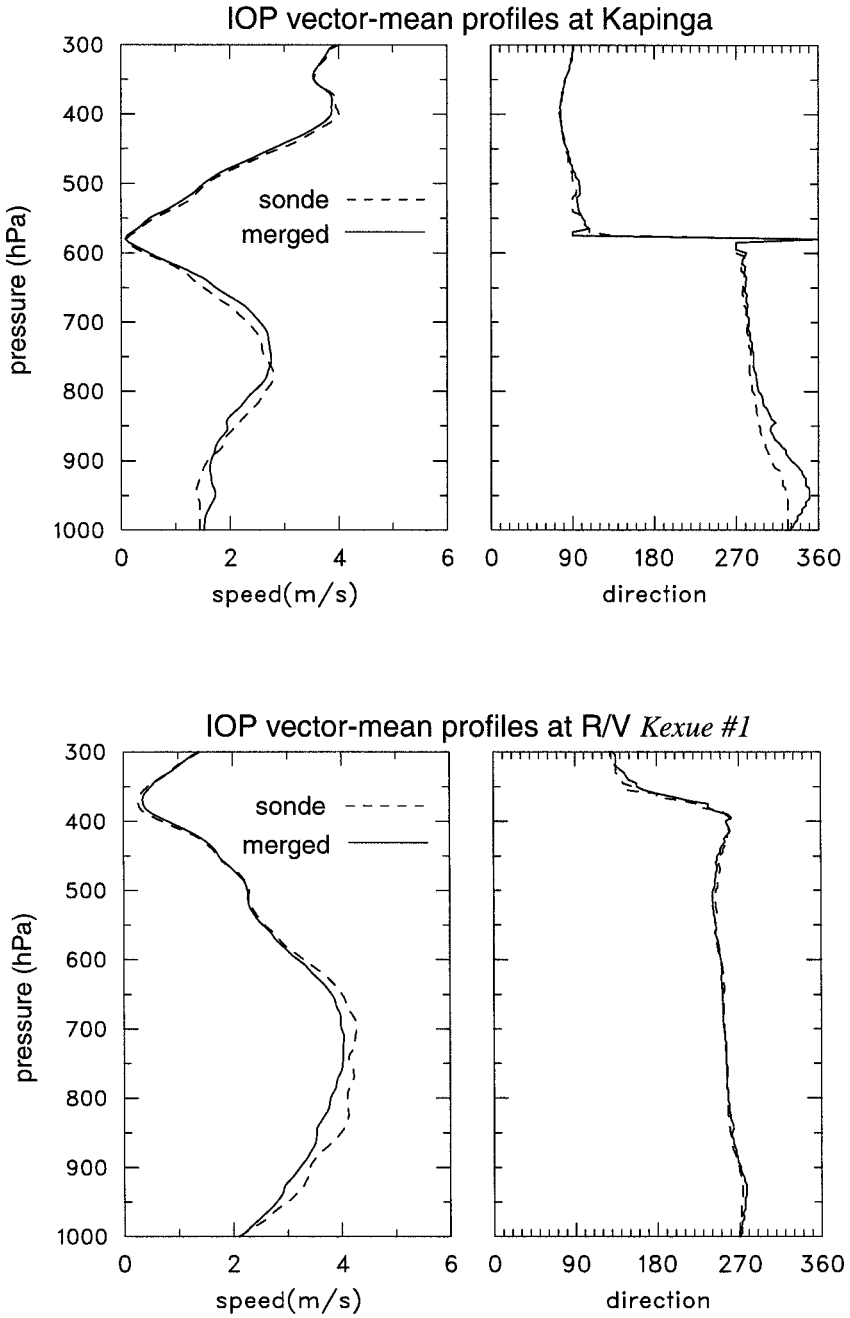

FIG. 6. The vector-mean wind speed and direction during the IOP at Kapinga (top panels) and at R/V *Kexue #1* (bottom panels). The solid line indicates merged data, while the dashed line is the interpolated sonde data; see text for details.

term mean at the ships, the merged profiles show decreased wind speeds (less than 1.0 m s^{-1}) below 600 hPa; directions have remained unchanged. At the land sites, the merge has increased speeds in the lowest 100 hPa and above 700 hPa with slight decreases between 700 and 900 hPa. The merge procedure has also resulted in mean wind direction profiles that have a stronger northerly component in the lower troposphere; this is especially evident in the lowest 100 hPa and at Kapinga.

At each time and location, the difference between the merged profile and the sonde profile can be calculated; this difference is referred here as the ''correction.'' The correction, if there is one, is due not only to the use of the profiler winds but also to the exclusion of interpolated sonde winds and to the use of a filter to smooth disjoint regions present after the merge. The mean corrections to the u and v components above 950 hPa were very similar at all stations, ranging from -1.1 to 0.4 m

s^{-1} and -0.7 to 0.2 m s^{-1}, respectively. Riddle et al. (1996) found mean profiler minus sonde differences ranging from -1.3 to 1.7 m s^{-1} and -0.9 to 0.9 m s^{-1} for the u and v components (A. Riddle 1996, personal communication). The maximum mean standard deviations of the corrections were 2.7 and 1.9 m s^{-1} for the u and v components, compared to 3.4 and 3.0 m s^{-1} standard deviations of profiler minus sonde data in Riddle et al. (1996). The smaller variances in our work are not surprising since the merged scheme used here in some rough sense ''splits the difference'' between the profiler and the sonde data.

The long-term means of the speed and direction corrections were computed but are not shown here. Speed correction profiles at all sites show sharp changes in the vertical gradient, accompanied by large variances and usually associated with correction maxima near 950 and 850 hPa. These are the levels near which high-resolution profiler data were first available at these sites (300–700 m) and at which low-resolution instead of high-resolution data were first used (≈1500 m). These features appear to be caused by the switch between different profiler resolutions.

5. Impacts of merged data

In this section we examine the impacts of using the merged data on various circulation fields and budget-derived precipitation. Sensitivity tests designed to gauge the impact of using the merged analyses are confined to areas in and near the IFA where the number of missing or bad sonde wind observations is largest (see Fig. 2). To facilitate this testing, objective analyses were performed on two datasets: a sonde-only dataset consisting of atmospheric observations from the network depicted in Fig. 1, and a merged dataset consisting of data from this same network except with merged winds at the ISS sites and Biak. In both datasets, unreliable winds or missing observations were filled in by interpolation at 25-hPa intervals from 1000 to 25 hPa. The data were then objectively analyzed at these pressure levels onto a 1° by 1° grid over an area larger than the LSA (20°S–20°N, 130°E–170°W) using multiquadric interpolation (Nuss and Titley 1994). In this manner, a sonde-only and a merged gridded analyses were generated at 6-h intervals for the entire 120-day IOP.

Budget-derived precipitation is diagnosed by vertically integrating the moisture budget equation:

$$Q_2 \equiv -L\left(\frac{\partial \overline{q}}{\partial t} + \overline{\mathbf{v}} \cdot \nabla \overline{q} + \overline{\omega}\frac{\partial \overline{q}}{\partial p}\right), \tag{3}$$

where Q_2 is the apparent moisture sink (Yanai et al. 1973), L is the latent heat of condensation, q is the specific humidity, and the overbar refers to a horizontal average. Integrating (3) from p_T (pressure at cloud top) to p_s (surface pressure) yields

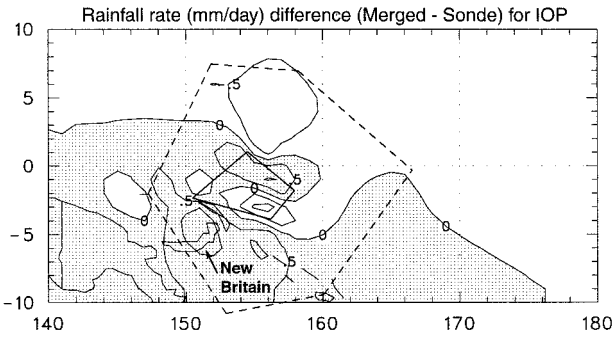

FIG. 7. IOP-mean rainfall rate difference (mm day^{-1}) between budget-derived estimates computed with merged analyses minus sonde-only analyses. Contour increment is 0.5 mm day^{-1}. The shading depicts the regions where the merged analyses resulted in increased rainfall.

$$P_o = \frac{1}{gL}\int_{p_T}^{p_s} Q_2 dp + E_o, \tag{4}$$

where P_o is precipitation rate, g is the gravitational constant, and E_o is the surface evaporation flux. In (3) the vertical motion ω is computed by integrating the mass continuity equation from the surface to 75 hPa. The vertical velocity was set to zero at this level by applying a constant adjustment to the vertical divergence profile (O'Brien 1970). Surface evaporation was estimated from ECMWF values adjusted by IFA buoy values with a procedure described in Lin and Johnson (1996).

Several methods exist for estimating surface rainfall, each having their own errors and inherent biases. A detailed comparison of these methods is beyond the scope of this paper. For this study we have chosen to assess the accuracy of the budget-derived rainfall rates by comparing them primarily to estimates derived from the Special Sensor Microwave/Imager (SSM/I). This is not to say that SSM/I provides the best estimates under all conditions; however, its spatial resolution (~45 km with a sampling frequency generally twice per day) and large-scale coverage make it a convenient dataset for comparison to our budget estimates. The SSM/I estimates used here (courtesy of G. Liu and J. Curry) are based on an algorithm that combines the scatter and emission information received by a microwave sensor from a polar-orbiting satellite and then integrates them through the troposphere (Liu and Curry 1992). To facilitate a comparison with the budget-derived rainfall estimates, the SSM/I measurements were mapped onto a 1° resolution grid over the LSA. The IOP-mean rainfall distribution over the LSA from SSM/I and budget estimates are shown in Lin and Johnson (1996). Basically these analyses show two east–west-oriented bands of heavy precipitation: one centered near 5°N and the other near 3°S but extending into the eastern IFA. During the IOP the heaviest rainfall rates (>18 mm day^{-1}) analyzed by the SSM/I occurred southwest of the IFA near the island of New Britain.

Figure 7 shows the impact of using the merged profiler

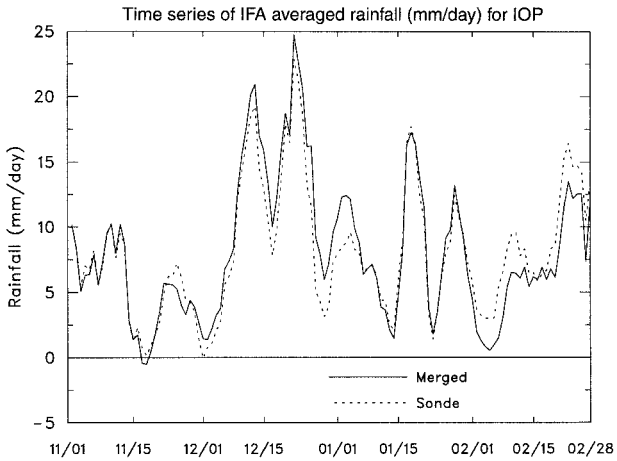

FIG. 8. Time series from 1 November 1992 to 28 February 1993 of IFA-averaged rainfall (mm day^{-1}) from budget-derived estimates (5-day running means) computed from the sonde-only analyses (dashed line) and the merged analyses (solid line).

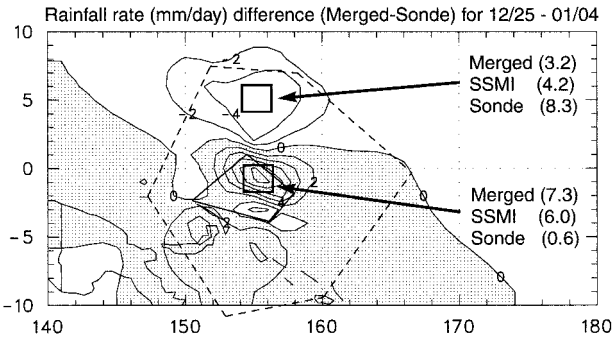

FIG. 9. Rainfall rate difference (mm day^{-1}) for the period 25 December 1992–4 January 1993 between budget-derived estimates computed with merged analyses minus sonde-only analyses. Contour interval is 2.0 mm day^{-1}. Shading depicts the regions where the merged analyses resulted in increased rainfall. The northern box centered at 4°N, 155°E and the southern box centered at 1°S, 155°E highlight the areas of extreme differences. Also shown here are the 11-day period rainfall averages over these areas from the SSM/I and the two analyses.

winds upon the IOP-mean rainfall over the LSA. In general, the merged analyses result in smaller rainfall rates over the northern and eastern LSA with larger rates to the south and west. In particular, rainfall rate increases of approximately 1 mm day^{-1} occur over the northern IFA and near New Britain, while a similar magnitude decrease exists over the southern IFA. Overall, the IOP-mean rainfall rate over the IFA changes only slightly from 8.1 mm day^{-1} in the sonde-only analyses to 8.2 mm day^{-1} in the merged analyses.[3] Although these IOP-mean differences are small, in general, they are the result of large deviations between the analyses that occur on timescales from a few days to a month. The time series of IFA-averaged rainfall (Fig. 8) from the two analyses show a substantial increase in IFA rainfall in the merged analyses during an 11-day period near the end of 1992. On the other hand, during much of February the merged analysis exhibits a significant decrease in IFA-averaged rainfall in comparison to the sonde-only analyses. We now examine these two periods when the analyses produced significantly different rainfall patterns.

The horizontal distribution of rainfall differences for the 11-day period from 25 December 1992 to 4 January 1993 (Fig. 9) shows a rainfall rate increase produced by the merged analysis of greater than 10 mm day^{-1} over the northeastern IFA, and a decrease of greater than 5 mm day^{-1} north of IFA. The 2° square boxes in Fig. 9 highlight these regions of extreme differences. Also shown in this figure are the 11-day rainfall rate averages from the SSM/I and the two analyses over the areas covered by the boxes. The large rainfall differences between the analyses are principally related to a significant loss of sonde wind data at Kapinga during this late December–early January period. Sonde winds were missing at this site more than 50% of the time below 700 hPa increasing to more than 80% below 850 hPa (Fig. 10). By merging in the profiler data, the mean wind profile at Kapinga (Fig. 11) changes substantially for this period. For example, between 950 and 650 hPa the westerly wind component decreases by approxi-

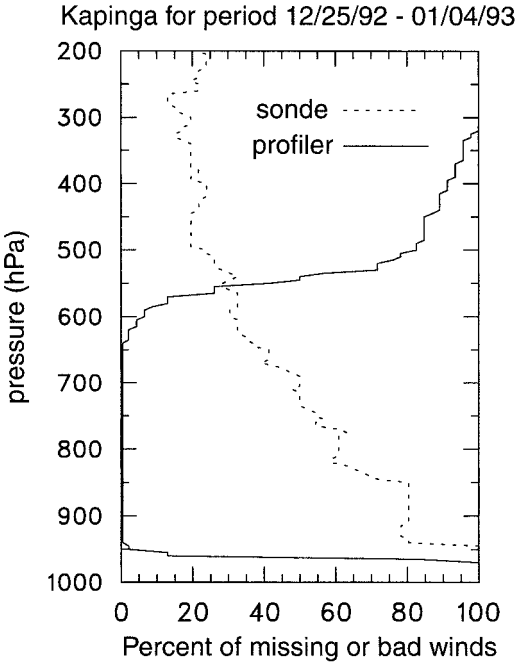

FIG. 10. Percent of missing observations in the sonde (dashed line) and profiler (solid line) datasets at Kapinga for the 11-day period from 25 December 1992–4 January 1993.

[3] A detailed comparison of rainfall estimates produced by various methods and platforms during the COARE IOP can be found in Bradley and Weller (1996).

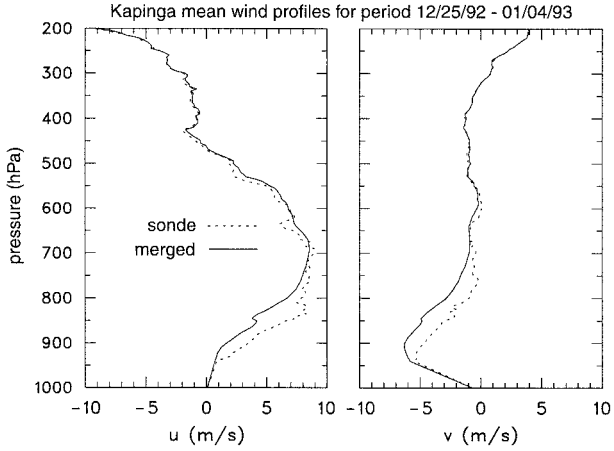

FIG. 11. Zonal and meridional wind profiles at Kapinga averaged over the period 25 December 1992–4 January 1993. Solid line results from using the merged dataset, while the dashed line results from using only sonde winds.

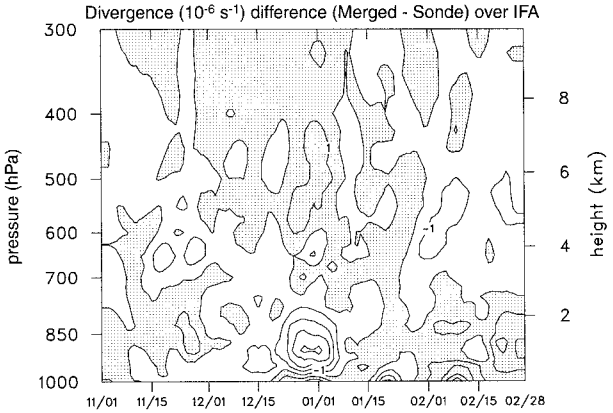

FIG. 13. Time series from 1 November 1992 to 28 February 1993 of IFA averaged divergence difference (10^{-6} s^{-1}) between merged analyses minus the sonde-only analyses. Contour interval is 1×10^{-6} s^{-1}. Differences represent 5-day running means. The shading depicts periods of increased divergence over the IFA in the merged analyses.

mately 3 m s^{-1}, while the northerly wind component increases by approximately 2 m s^{-1} in the merged profiles. The strong low-level westerlies seen here are a signature of a major westerly wind burst event that was present over IFA (Gutzler et al. 1994; Velden and Young 1994). The horizontal extent of the westerly burst as it appeared in the sonde-only and merged analyses at 850 hPa on 29 December 1992 is shown in Fig. 12. At this pressure level the westerly wind component at Kapinga is nearly 10 m s^{-1} less in the merged analyses (see also Fig. 5). This reduction along with some smaller wind changes at other ISS sites results in a more spatially coherent westerly wind maximum south of equator in the merged analyses. The wind changes at Kapinga depicted in Fig. 11 result in circulation changes over the IFA in the merged analyses, namely, increased low-level convergence (Fig. 13) and upward vertical motion (Fig. 14) and, consequently, increased rainfall. Conversely, in the region north of the IFA low-level convergence and upward vertical motion are decreased, resulting in a reduced rainfall rate in the merged analyses. In the Tropics, storage and horizontal variations of q are small, so that the vertical advection term in (3) is a dominant contributor to Q_2 and hence P_o in convective situations.

Inspection of the area-average rainfalls shown in Fig. 9 suggests that the inclusion of profiler winds has im-

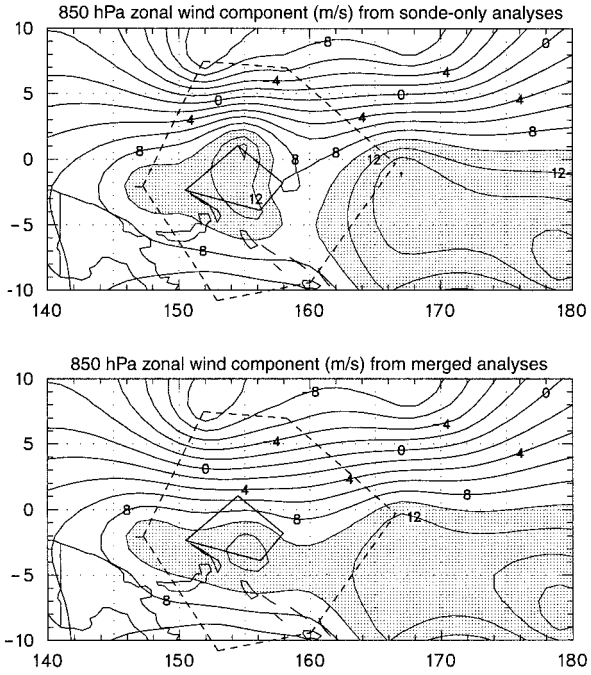

FIG. 12. Zonal wind component (m s^{-1}) at 850 hPa over the LSA at 1200 UTC 29 December 1992 from the sonde-only (top panel) and merged analyses (bottom panel). Contour interval is 2 m s^{-1} with westerlies over 10 m s^{-1} shaded.

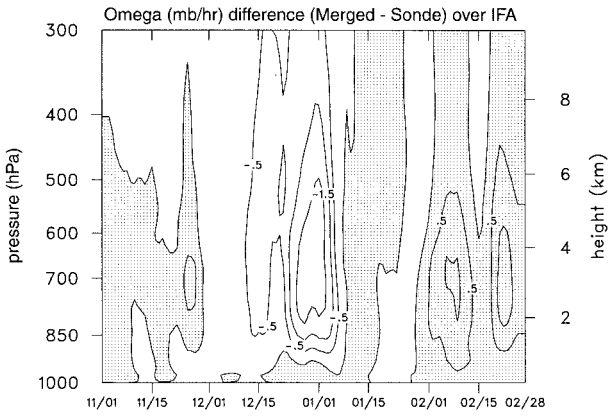

FIG. 14. Time series from 1 November 1992 to 28 February 1993 of IFA-averaged vertical motion difference (mb h^{-1}) between merged analyses minus the sonde-only analyses. Differences represent 5-day running means. Contour interval is 0.5 mb h^{-1}. The shading depicts periods of increased subsidence over the IFA in the merged analyses.

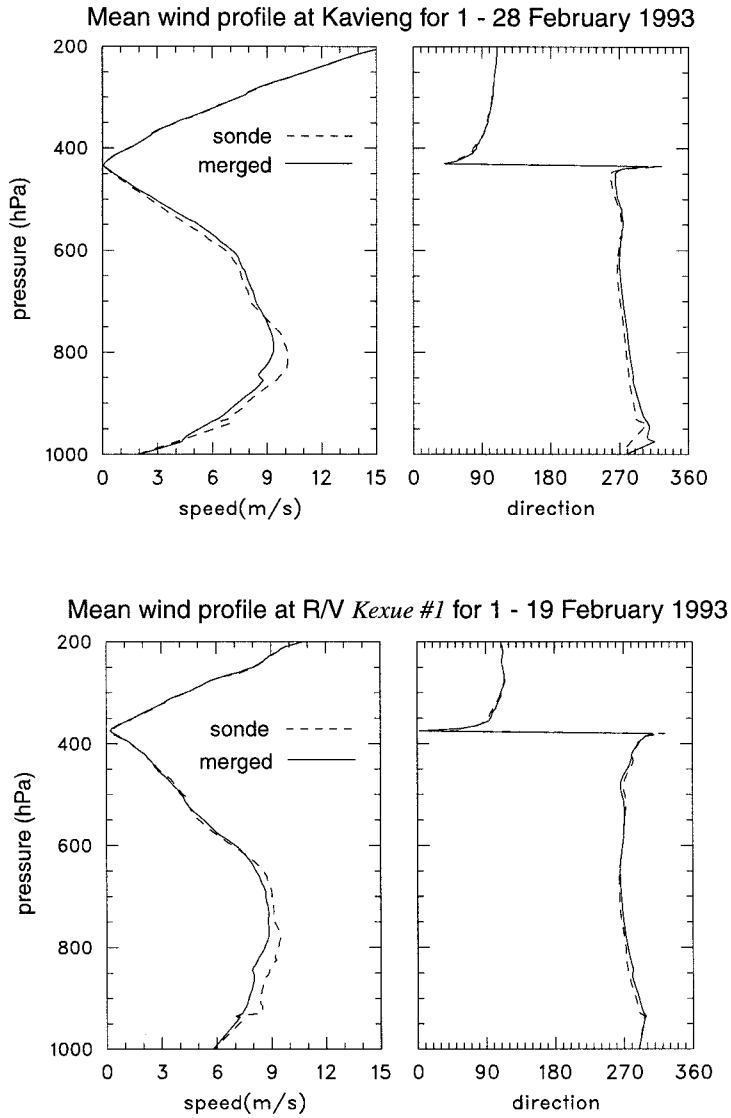

FIG. 15. Wind speed and direction profiles at Kavieng (top panels) averaged from 1 to 28 February 1993, and at R/V *Kexue #1* (bottom panels) averaged from 1 to 19 February 1993. The solid line results from using the merged dataset, while the dashed line results from using only sonde winds.

proved the analyses. For example, the average budget-derived rainfall was within 1.0 mm day^{-1} (1.3 mm day^{-1}) of the SSM/I estimate for the merged analyses compared to 4.1 mm day^{-1} (5.3 mm day^{-1}) for the sonde-only analyses for the northern (southern) area. Further confirmation that the derived rainfall estimate from the merged analyses in the southern area of 7.3 mm day^{-1} is an improvement comes from two nearby ships. For the 11-day period in question, the estimate from the MIT radar on the R/V *Vickers* (2°S, 156°E) was 5.0 mm day^{-1} (T. Rickenbach 1995, personal communication), while the optical rain gauge on R/V *Shiyan #3* (2.2°S, 157.9°E) recorded an averaged rain rate of 7.5 mm day^{-1}. The merged analyses also eliminates the unrealistic negative precipitation rates[4] present on 3 of the 11 days in the daily rainfall time series (not shown) from the sonde-only analyses over the southern area. The average rainfall rate for these 3 days is -10.7 mm day^{-1} in the sonde-only analyses and -0.16 mm day^{-1} in the merged analyses.

[4] Negative precipitation rates associated with the analyses result from a combination of factors: sampling errors (i.e., the inadequacy of a sounding at a given location and time to represent conditions in a larger area and a longer time period), data errors, errors introduced by the objective analyses, and errors in the estimation of the surface flux E_o.

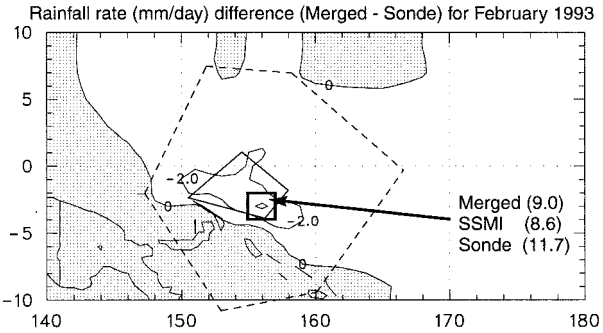

FIG. 16. Rainfall rate difference (mm day^{-1}) for February 1993 between budget-derived estimates computed with merged analyses minus sonde-only analyses. Contour interval is 2.0 mm day^{-1}. Shading depicts the regions where the merged analyses resulted in increased rainfall. The box centered at 3°S, 156°E highlights the area of extreme differences. Also shown are the mean February rainfall amounts averaged over this area from the SSM/I and the two analyses.

The rainfall reduction observed over the IFA in the merged analyses during much of February (cf. Fig. 8) is directly related to increases in low-level divergence (Fig. 13) and subsidence (Fig. 14) in the merged analyses during this period. This increase in low-level divergence is the result of some small, but subtle wind differences between the datasets, primarily at Kavieng and R/V *Kexue #1*. Figure 15 shows the mean February wind profiles from the sonde-only and merged datasets at these two sites. From these profiles it would appear that the increased low-level divergence over the IFA in the merged analyses during February results from insignificant dataset differences in the wind at R/V *Shiyan #3* (not shown) coupled with reduced low-level westerlies in the merged data at the sites shown in Fig. 15. During the first 19 days of February when the ships were present over the IFA, the increased low-level divergence is confined to the southern IFA. However, after the ships leave, the influence radius of Kavieng's winds increases such that the merged analyses exhibit increased low-level divergence over the entire IFA. The horizontal distribution of rainfall differences for February (Fig. 16) favors the period when the ships were present, showing a rainfall reduction produced by the merged analysis of greater than 2 mm day^{-1} over the southern IFA. The area of maximum rainfall reduction of greater than 4 mm day^{-1} is highlighted with a box in Fig. 16. Over this highlighted area the difference between the merged and SSM/I estimates is only 0.4 mm day^{-1} compared to a difference of 3.1 mm day^{-1} between the sonde-only and SSM/I estimates. Thus, as in the previous case, the inclusion of profiler winds into a merged dataset appears to have improved the analyses.

Finally, we consider the validity of the IOP-mean rainfall increase near New Britain in Fig. 7. Whereas the IOP-mean rainfall differences for the areas discussed above are accounted for primarily by the large analyses changes on a timescale of a few weeks to a month, the increase near New Britain results from several shorter episodes of moderate rainfall increase in the merged analyses. The IOP-mean rainfall rate from SSM/I for a 2° square area centered at 4°S, 151°E (i.e., near the maximum in rainfall increase near New Britain) is 12.1 mm day^{-1}. The budget-derived estimates for this same region are 8.1 and 9.2 mm day^{-1} from the sonde-only and merged analyses, respectively. This rainfall increase produced by the merged analyses near New Britain further corroborates the notion that inclusion of profiler winds has benefited the analyses.

6. Concluding remarks and dataset availability

Achieving many of the COARE objectives is contingent on the availability of a high-quality atmospheric sounding dataset. Despite the enormous effort to achieve this goal, deficiencies still exist in the upper-air sounding dataset. For example, at the ISS sites good sonde launches on the average contained missing or bad wind data approximately 20% of the time below 500 hPa and approximately 45% of the time below 800 hPa. This study attempts to minimize these deficiencies by merging together winds from collocated rawinsonde and profiler soundings at six ISS sites and Biak. Four of these ISS sites, which are located on the vertices of the IFA, formed the nucleus of the atmospheric observing network for TOGA COARE.

A simple procedure, which uses data quality information, was designed to merge the rawinsonde and profiler winds into a single coherent dataset. This merge procedure yields IOP-mean wind profiles consistent with earlier studies. These mean merged soundings exhibit some systematic differences from soundings constructed from the sonde-only dataset. On the ships, the mean merged profiles have low and midtropospheric vector-mean wind speeds up to 1 m s^{-1} weaker than do the sonde profiles without any systematic differences in direction. Over the land stations, the merged winds are generally stronger and more northerly in the lowest 100 hPa, weaker between 700 and 900 hPa, and stronger than the sonde profiles through the rest of the troposphere.

The favorable agreement between IOP-mean profiles of sonde and profiler winds gave us confidence to use profiler winds in absence of, or in combination with, sonde winds. As a result, numerous data gaps due to sonde tracking problems or sonde launches that were completely missed (or prematurely terminated) were eliminated through use of profiler wind data. In situations where sonde tracking problems occurred, the merge procedure was able to detect poor quality or missing sonde winds and generate a more realistic wind profile. Using our merge procedure the amount of missing or bad winds was reduced from approximately 20% to approximately 10% below 500 hPa and from approximately 45% to less than 20% below 800 hPa at the land-based ISS sites. At the ship-based ISS sites these reductions were smaller due to less reliable profiler winds below 700 m.

To gauge the impact of merging profiler winds into the rawinsonde dataset, we objectively analyzed the sonde-only and the merged datasets and then compared various circulation fields and budget-derived precipitation from the two analyses. These sensitivity tests were confined to areas

in and near the IFA where the number of missing or bad sonde wind observations is largest. To assess whether the changes brought about by the inclusion of the profiler winds were an improvement to the analyses, we compared budget-derived rainfall estimates to those provided by the SSM/I. Time series of IFA-averaged budget-derived rainfall for the two analyses show large differences for two periods: the first during a strong westerly wind burst event near the end of 1992 and the second during most of February 1993. During this former period, more than half of the sonde winds were missing at Kapinga below 700 hPa. Utilizing profiler winds caused an increase in low-level northerlies at Kapinga during this period, resulting in increased low-level convergence and, hence, upward vertical motion and precipitation over the northern IFA. Conversely, a decrease in these derived fields was observed to the north of the IFA. Both of these rainfall tendencies in the merged analyses are consistent with SSM/I estimates. During most of February 1993 the merged analyses showed a reduction of precipitation over the IFA. This rainfall decrease, which was a consequence of increased low-level divergence in the merged analyses, was again consistent with SSM/I observations. These comparisons along with other sensitivity tests presented in the paper suggest that merging profiler winds into the sonde dataset has a beneficial impact upon the analyses.

The merged datasets for the seven sites described herein are available through anonymous ftp to tornado.atmos.colostate.edu in directory dist/toga/merged_data. A README file in this directory describes the organization and format of the data, as well as many of the technical details presented here. This same information is also available via the WWW using the JOSS data management system (CODIAC). The CODIAC–WWW interface for TOGA COARE data can be accessed from http://www.joss.ucar.edu/codiac/ by following the appropriate links to the TOGA COARE datasets.

Acknowledgments. Special thanks go to Scot Loehrer, Hal Cole, Eric Miller, and Dave Parsons for discussions that clarified many aspects of the OMEGA sonde system and the postprocessing of the sonde data, and Wayne Angevine, Paul Johnston, and Tony Riddle for similar discussions regarding the profiler data. In addition, we thank Xin Lin and Jim Bresch for their considerable contributions to the data analyses and Wayne Schubert for his insights and suggestions. Special appreciation is extended to Peter Webster and Roger Lukas for their exceptional efforts in conceiving, planning, and implementing TOGA COARE. This work was supported by the National Oceanic and Atmospheric Administration under Grants NA90RAH00077 and NA37RJ0202. In addition, one of the authors (LMH) has been supported by the U.S. TOGA Project Office through grants to the NOAA Aeronomy Laboratory.

REFERENCES

Bradley, E. F., and R. A. Weller, 1995: Joint Workshop of the TOGA COARE Flux and Atmospheric Working Groups. 35 pp. [Available from TOGA COARE International Project Office, UCAR, P.O. Box 3000, Boulder, CO 80307.]

——, and ——, 1996: Fourth Workshop of the TOGA COARE Air-Sea Interaction (Flux) Working Group. [Available from TOGA COARE International Project Office, UCAR, P.O. Box 3000, Boulder, CO 80307.]

Carter, D. A., K. S. Gage, W. L. Ecklund, W. M. Angevine, P. E. Johston, A. C. Riddle, J. Wilson, and C. R. Williams, 1995: Developments in UHF lower tropospheric wind profiling at NOAA's Aeronomy Laboratory. *Radio Sci.*, **30,** 977–1001.

Daley, R., 1991: *Atmospheric Data Analysis.* Cambridge University Press, 457 pp.

Franklin, J. L., and P. R. Julian, 1985: An investigation of OMEGA windfinding accuracy. *J. Atmos. Oceanic Technol.*, **2,** 212–231.

Gutzler, D. S., and L. M. Hartten, 1995: Daily variability of lower tropospheric winds over the tropical western Pacific. *J. Geophys. Res.*, **100,** 22 999–23 008.

——, G. N. Kiladis, G. A. Meehl, K. M. Weickmann, and M. Wheeler, 1994: Seasonal climate summary: The global climate of December 1992–February 1993. Part II: Large-scale variability across the tropical western Pacific during TOGA COARE. *J. Climate*, **7,** 1606–1622.

Hartten, L. M., 1997: Reconciliation of surface and profiler winds at ISS sites. *J. Atmos. Oceanic Technol.*, in press.

Lin, X., and R. H. Johnson, 1996: Heating, moistening and rainfall analyses over the western Pacific warm pool during TOGA COARE. *J. Atmos. Sci.*, **53,** 3367–3383.

Liu, W. T., and J. A. Curry, 1992: Retrieval of precipitation from satellite microwave measurements using both emission and scattering. *J. Geophys. Res.*, **97,** 9959–9974.

Loehrer, S. M., T. A. Edmands, and J. A. Moore, 1996: TOGA COARE upper-air sounding data archive: Development and quality control procedures. *Bull. Amer. Meteor. Soc.*, **77,** 2651–2671.

Miller, E. R., 1993: TOGA COARE intergrated sounding system data report—Volume 1, Surface and sounding data. Surface and Sounding Systems Facility, National Center for Atmospheric Research, 41 pp. [Available from TOGA COARE International Project Office, UCAR, P.O. Box 3000, Boulder, CO 80307-3000.]

——, and A. C. Riddle, 1994: TOGA COARE integrated sounding system data report. Vol. 1A, revised edition. National Center for Atmospheric Research, 61 pp. [Available from TOGA COARE International Project Office, UCAR, P.O. Box 3000, Boulder, CO 80307-3000.]

Nuss, W. A., and D. W. Titley, 1994: Use of multiquadric interpolation for meteorological objective analysis. *Mon. Wea. Rev.*, **122,** 1611–1631.

O'Brien, J. J., 1970: Alternative solutions to the classical vertical velocity problem. *J. Appl. Meteor.*, **9,** 197–203.

Parsons, D. B., and Coauthors, 1994: The integrated sounding system: Description and preliminary observations from TOGA COARE. *Bull. Amer. Meteor. Soc.*, **75,** 553–567.

Riddle, A. C., and E. R. Miller, 1994: TOGA COARE integrated sounding system data report—Vol. 16: Wind profiler and RASS at R/V *Moana Wave.* National Center for Atmospheric Research, Boulder, CO, 99 pp. [Available from TOGA COARE International Project Office, UCAR, P.O. Box 3000, Boulder, CO 80307.]

——, W. M. Angevine, W. L. Ecklund, E. R. Miller, D. B. Parsons, D. A. Carter, and K. S. Gage, 1996: In situ and remotely sensed horizontal winds and temperature intercomparisons obtained using integrated sounding systems during TOGA COARE. *Contrib. Atmos. Phys.*, **69,** 49–61.

Velden, C. S., and J. A. Young, 1994: Satellite observations during TOGA COARE: Large-scale descriptive overview. *Mon. Wea. Rev.*, **122,** 2426–2441.

Webster, P. J., and R. Lukas, 1992: TOGA COARE: The Coupled Ocean–Atmosphere Response Experiment. *Bull. Amer. Meteor. Soc.*, **73,** 1377–1416.

Yanai, M., S. Esbensen, and J. H. Chu, 1973: Determination of bulk properties of tropical cloud clusters form large-scale heat and moisture budgets. *J. Atmos. Sci.*, **30,** 611–627.